GSA DATA REPOSITORY 2013153 J.M. González-Jiménez et al.

References for Figure 1

Supecontinent Cycles

Columbia/Nuna (~1.8–1.5 Ga)

Zhao, G., Cawood, P.A., Wilde, S.A., Sun, M., 2002, Review of global 2.1–1.8 Ga orogens: implications for a pre-Rodinia supercontinent: Earth Science Reviews, v 59, p. 125–162.

Zhao, G., Sun, M., Wilde, S.A., Li, S.Z., 2004, A Paleo-Mesoproterozoic supercontinent: assembly, growth and breakup: Earth Science Reviews, v. 67, p. 91–123.

Rodinia (~1.1–0.75 Ga)

Torsvik, T.H., 2003, The Rodinia jigsaw puzzle: Science, v. 300, p. 1379–1381.

Cawood, P.A., 2005, Terra Australis Orogen: Rodinia breakup and development of the Pacific and Iapetus margins of Gondwana during the Neoproterozoic and Paleozoic: Earth-Science Reviews, v. 69, p. 249-279.

Gondwana (~ 0.5-0.65 Ga)

Cawood, P.A., 2005, Terra Australis Orogen: Rodinia breakup and development of the: Pacific and Iapetus margins of Gondwana during the Neoproterozoic and Paleozoic: Earth-Science Reviews, v. 69, p. 249-279.

Veevers, J.J. 2007. Pan-Gondwanaland post-collisional extension marked by 650-500 Ma alkaline rocks and carbonatites and related detrital zircons: A review: Earth Science Reviews, v. 83, p. 1-47.

Pangea (~380–180 Ma)

Cawood, P.A., Buchan, C., 2007, Linking accretionary orogenesis with supercontinent assembly: Earth Science Reviews, v. 82, p. 217–256.

Dunn, A.M., Reynolds, P.H., Clarke, D.B., Ugidos, J.M.,1998, A comparison of the age and composition of the Sherburne Dyke, Nova Scotia, and the Messejana Dyke, Spain. Canadian Journal of Earth Sciences, v. 35, p. 1110-1115.

Keppie, J.D., Nance, R.D., Murphy, J.B., Dostal, J., Braid, J., 2010, The high-pressure Iberian Czech belt in the Variscan orogen: extrusion into the upper (Gondwanan) plate?: Gondwana Research, v. 17, p. 306-316.

Ribeiro, A., Munhá, J., Fonseca, P.E., Araújo, A., Pedro, J.C., Mateus, A., Tassinari, C., Machado, G., Jesus, A., 2010, Variscan ophiolite belts in the Ossa-Morena Zone (southwest Iberia): geological chracterization and geodynamic significance: Gondwana Research, v. 17, p. 408-421

Orejana, D., Villaseca, C., Billstöm, Paterson, B.A., 2008, Petrogenesis of Permian alkaline lamprophyres and diabases from the Spanish Central System and their geodynamic context within western Europe: Contributions to Mineralogy and Petrology, v.156, p. 477-500.

<u>Re-Os data</u>

Calatrava (Spain)

[*In-situ LA-MC-ICPMS on individual sulfides*]

This study (results listed in Table DR1)

Massif Central (France)

[*In-situ LA-MC-ICPMS on individual sulfides*]

Alard, O., Griffin, W.L., Pearson, N.J., Lorand, J.P., O'Reilly, S.Y., 2002, New insights into the Re-Os systematics of sub-continental lithospheric mantle from in situ analysis of sulphides: Earth Planetary Science Letters, v. 203, p. 651-663.

[*N-TIMS on mineral separates and sulfides*]

Harvey, J., Gannoun, A., Burton, K.W., Schiano, P., Rogers, N.W., Alard, O., 2010, Unravelling the effests of melt depletion and secondary infiltration on mantle re-Os isotopes beneath the French Massif Central: Geochimica et Cosmochimica Acta, v. 74, p. 293-320.

[*Whole-rock*]

Meisel, T., Richard, J.W., Irving, A.J., Lorand, JP, 2001, Osmium isotopic compositions of mantle xenoliths: A global perspective: Geochimica et Cosmochimica Acta, v. 65, p. 1311-1323.

Languedoc (France)

[*In-situ LA-MC-ICPMS on individual sulfides*]

Alard, O., Griffin, W.L., Pearson, N.J., Lorand, J.P., O'Reilly, S.Y., 2002, New insights into the Re-Os systematics of sub-continental lithospheric mantle from in situ analysis of sulphides: Earth Planetary Science Letters, v. 203, p. 651-663.

Bohemian Massif (Czech Republic)

[*Whole-rock*]

Ackerman, L., Pircher, L., Strnad, L., Putchel, I.S., Jelinek, E., Walker, R.J., Rohovec, J., 2012, Highly siderophile element geochemistry of peridotites and pyroxenites from Horní Bory, Bohemian Massif: implications for HSE behavior in subduction-related upper mantle. Geochimica et Cosmochimica Acta, http://dx.doi.org/10.1016/j.gca.2012.09.050.

Rhenish Massif (Germany)

[*Whole-rock*]

Meisel, T., Richard, J.W., Irving, A.J., Lorand, J.-P, 2001, Osmium isotopic compositions of mantle xenoliths: A global perspective: Geochimica et Cosmochimica Acta, v. 65, p. 1311-1323.
Schmidt, G., and Snow, J., 2002, Os isotopes in mantle xenoliths from the Eifel volcanic field and the Vogelsberg (Germany): age constrains on the lithospheric mantle: Contributions to Mineralogy and Petrology, v. 143, p. 694-705.

Pyrenees (France)

[*Whole-rock*]

Reisberg, L. C., and Lorand, J.-P, 1995, Longevity of sub-continental mantle lithosphere from osmium isotope systematics in orogenic peridotite massifs. Nature, v. 376, 159-162.

Azrou (France)

[*Whole-rock*]

Wittig, N., Pearson, D.G., Baker, J.A., Duggen, S., Hoernle, K., 2010, A major element, PGE and Re-Os isotope study of Middle-Atlas (Morocco) peridotite xenoliths: Evidence for coupled introduction of metasomatic sulphides and clinopyroxene: Lithos, v. 115, p. 15-26.

References for Figure 2

El Aprisco (Calatrava, Spain)

[*In-situ LA-MC-ICPMS on individual sulfides*]

This study (results listed in Table DR1)

Massif Central (France)

[*In-situ LA-MC-ICPMS on individual sulfides*]

Alard, O., Griffin, W.L., Pearson, N.J., Lorand, J.P., O'Reilly, S.Y., 2002, New insights into the Re-Os systematics of sub-continental lithospheric mantle from in situ analysis of sulphides: Earth Planetary Science Letters, v. 203, p. 651-663.

[*N-TIMS on mineral separates and sulfides*]

Harvey, J., Gannoun, A., Burton, K.W., Schiano, P., Rogers, N.W., Alard, O., 2010, Unravelling the effests of melt depletion and secondary infiltration on mantle re-Os isotopes beneath the French Massif Central: Geochimica et Cosmochimica Acta, v. 74, p. 293-320.

[*Whole-rock*]

Meisel, T., Richard, J.W., Irving, A.J., Lorand, JP, 2001, Osmium isotopic compositions of mantle xenoliths: A global perspective: Geochimica et Cosmochimica Acta, v. 65, p. 1311-1323.

Languedoc (France)

[*In-situ LA-MC-ICPMS on individual sulfides*]

Alard, O., Griffin, W.L., Pearson, N.J., Lorand, J.P., O'Reilly, S.Y., 2002, New insights into the Re-Os systematics of sub-continental lithospheric mantle from in situ analysis of sulphides: Earth Planetary Science Letters, v. 203, p. 651-663.

Bohemian Massif (Czech Republic)

[*Whole-rock*]

Ackerman, L., Pircher, L., Strnad, L., Putchel, I.S., Jelinek, E., Walker, R.J., Rohovec, J., 2012, Highly siderophile element geochemistry of peridotites and pyroxenites from Horní Bory, Bohemian Massif: implications for HSE behavior in subduction-related upper mantle. Geochimica et Cosmochimica Acta, http://dx.doi.org/10.1016/j.gca.2012.09.050.

Rhenish Massif (Germany)

[*Whole-rock*]

Meisel, T., Richard, J.W., Irving, A.J., Lorand, J.-P, 2001, Osmium isotopic compositions of mantle xenoliths: A global perspective: Geochimica et Cosmochimica Acta, v. 65, p. 1311-1323.

Schmidt, G., and Snow, J., 2002, Os isotopes in mantle xenoliths from the Eifel volcanic field and the Vogelsberg (Germany): age constrains on the lithospheric mantle: Contributions to Mineralogy and Petrology, v. 143, p. 694-705.

Pyrenees (France)

[*Whole-rock*]

Reisberg, L. C., and Lorand, J.-P, 1995, Longevity of sub-continental mantle lithosphere from osmium isotope systematics in orogenic peridotite massifs. Nature, v. 376, 159-162.

Azrou (Morocco)

[*Whole-rock*]

Wittig, N., Pearson, D.G., Baker, J.A., Duggen, S., Hoernle, K., 2010, A major element, PGE and Re-Os isotope study of Middle-Atlas (Morocco) peridotite xenoliths: Evidence for coupled introduction of metasomatic sulphides and clinopyroxene: Lithos, v. 115, p. 15-26.

Beni Boussera (Morocco)

[*Whole-rock*]

Pearson, D.G., and Nowell, G.M., 2004, Re-Os and Lu-Hf isotope constraints on the origin and age of pyroxenites from the Beni Bousera peridotite massif implications for mixed peridotitepyroxenite mantle sources: Journal of Petrology, v. 45, p. 439–455.

Ronda (Spain)

[*In-situ LA-MC-ICPMS on individual sulfides*]

Marchesi, C.,Griffin, W.L., Garrido, C.J., Bodinier, J.-L., O'Reilly, S.Y., Pearson, N.J., 2010, Persistence of mantle lithospheric Re-Os signature during asthenospherization of the subcontinental lithospheric mantle: insights from in situ isotopic analysis of sulfides from the Ronda peridotite (southern Spain): Contributions to Mineralogy and Petrology, v. 159, p 315-330.

Ojén (Spain)

[*In-situ LA-MC-ICPMS on individual sulfides*]

González-Jiménez, J.M., Marchesi, C., Griffin, W.L., Gutiérrez-Narbona, R., Lorand, J.-P., O'Reilly, S., Garrido, C.J., Gervilla, F., Pearson, N.J., Hidas, K., 2012, Transfer of Os isotopic signatures from peridotite to chromitite in the subcontinental mantle: insights from *in situ* analysis of platinum-group and base-metal minerals (Ojén peridotite massif, southern Spain): Lithos, doi:10.1016/j.lithos.2012.07.009.

Tallante (Spain)

[*In-situ LA-MC-ICPMS on individual sulfides*]

Konc, Z., Marchesi, C., Garrido, C.J., González-Jiménez, J.M., Griffin, W.L., Alard, O., Hidas, K., O'Reilly, S.Y., Pearson, N.J., 2012, Provenance and evolution of the western Mediterranean lithospheric mantle beneath the eastern Betics (S. Spain): insights from in-situ analyses of Os isotopes and platinum-group elements in sulphides from the Tallante mantle xenoliths: Geophysical Research Abstracts, v. 15, EGU2012-12929.

Sicily (Italy)

[*In-situ LA-MC-ICPMS on individual sulfides*]

Sapienza, G.T., Griffin, W.L., O'Reilly, S.Y., Morten, L., 2007, Crustal zircons and mantle sulfies: Archean to Triassic events in the lithosphere beneath south-eastern Sicily: Lithos, v. 96, 503-523.

Liguride (Italy)

[*In-situ LA-MC-ICPMS on individual sulfides*]

Alard, O., Luguet, A., Pearson, N.J., Griffin, W.L., Lorand, J.-P., Gannoun, A., Burton, K.W., O'Reilly, S.Y., 2005, In-situ Os isotopes in abyssal peridotites bridge the isotopic-gap between MORBs and their source mantle. Nature, v. 436, p. 1005–1008.

Kraubath (Austria)

[*In-situ LA-MC-ICPMS on individual sulfides*]

Malitch, K.N., 2004, Osmium isotope constraints on contrasting sources and prolonged melting in the Proterozoic upper mantle: evidence from ophiolitic Ru–Os sulfides and Ru–Os–Ir alloys: Chemical Geology, v. 208, p. 157-173.

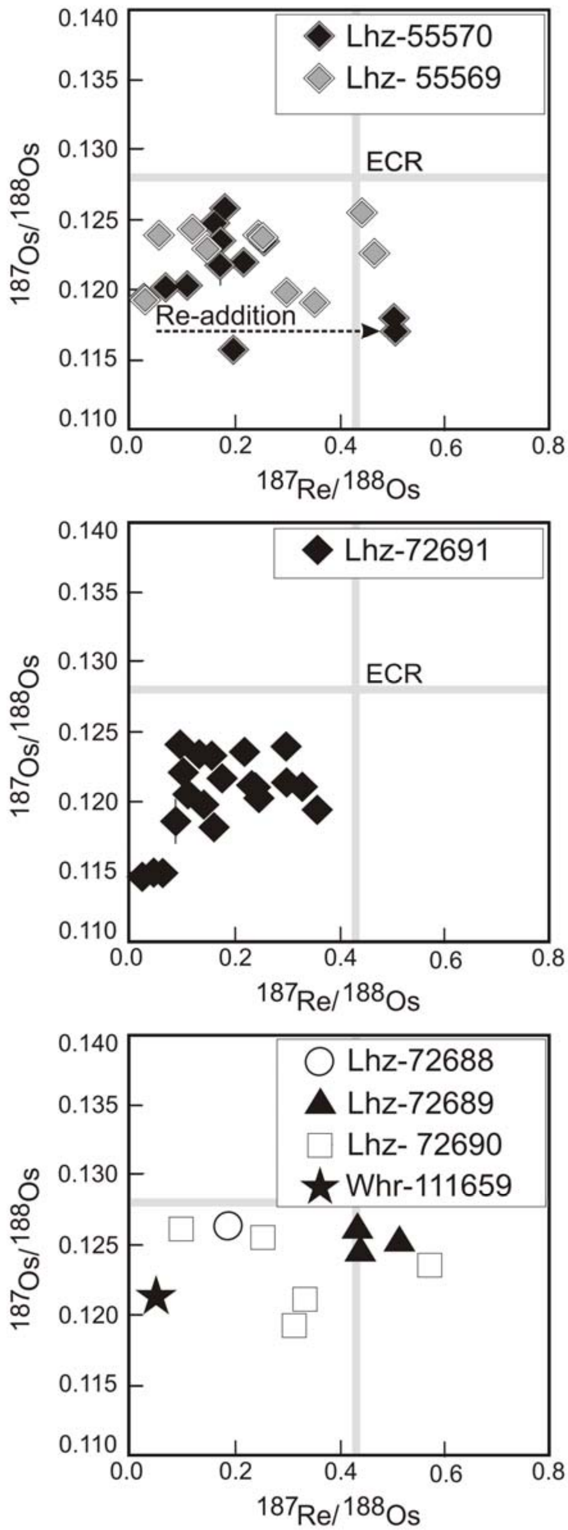

Figure DR1. Plots of $^{187}Re/^{188}Os$ versus $^{187}Os/^{188}Os$ for sulfides of the El Aprisco peridotite xenoliths). Note that uncertainties (2SE) are presented as bars but in most cases they are smaller than symbols sizes. ECR correspond to values of the Enstatitic Chondritic Reservoir (Walker et al., 2002). Legend inset: Lhz: lherzolite; Whr: wehrlite, numbers refer to the sample labeling of Villaseca et al. (2010)].

Table DR1. Re-Os isotopic compositions ofsulfides from peridotite xenoliths of the Calatrava Volcanic Field

	Mophology	host	$^{187}Os/^{188}Os$	2σ	$^{187}Re/^{188}Os$	2σ	Os[a] ppm	2σ	Pt[a] ppm	2σ	Re/Os	γOs^{ECR}	T_{Ma}^{ECR}(Ga)	2σ (Ga)	T_{RD}^{ECR} (Ga)	2σ (Ga)
Sample-55569																
1	Subhedral	Clinopyroxene-1	0.1191	0.0014	0.0241	0.0032	31.5	4.8	10.6	2.0	0.01	-7.0	***1.35***	0.21	***1.27***	0.20
2	Euhedral	Clinopyroxene-1	0.1237	0.0014	0.0549	0.0036	29.4	5.2	7.1	0.9	0.01	-3.4	***0.71***	0.22	***0.62***	0.19
3	Subhedral	Clinopyroxene-1	0.1230	0.0008	0.1450	0.0036	52.9	3.1	43.6	1.0	0.03	-4.0	1.10	0.18	0.72	0.12
4	Subhedral	Clinopyroxene-1	0.1237	0.0007	0.2548	0.0112	35.9	3.2	58.5	1.4	0.06	-3.5	1.58	0.25	0.63	0.09
5	Euhedral	Olivine	0.1255	0.0009	0.4450	0.0156	20.3	2.4	13.7	1.0	0.10	-2.0	-6.95	5.35	0.37	0.12
6	Anhedral	Interstitial glass	0.1242	0.0004	0.1169	0.0058	67.6	8.4	5.0	0.4	0.03	-3.1	**0.77**	0.07	**0.55**	0.05
7	Anhedral	Interstitial glass	0.1197	0.0008	0.2993	0.0178	51.5	2.0	12.5	0.1	0.07	-6.5	4.00	0.67	**1.18**	0.11
8	Anhedral	Interstitial glass	0.1190	0.0008	0.3495	0.0300	42.8	4.4	10.5	0.7	0.08	-7.1	7.20	2.91	**1.28**	0.11
10	Anhedral	Interstitial glass	0.1238	0.0012	0.2474	0.0140	26.8	3.6	9.7	1.3	0.06	-3.4	**1.48**	0.41	**0.61**	0.16
11	Anhedral	Interstitial glass	0.1226	0.0008	0.4649	0.0040	55.7	1.6	4.5	0.2	0.10	-4.3	-7.97	1.45	**0.77**	0.11
Sample-55570																
1	Euhedral	Clinopyroxene-1	0.1195	0.0008	0.0215	0.0038	29.9	4.8	10.0	1.8	0.00	-6.7	***1.27***	0.12	***1.21***	0.12
2	Subhedral	Clinopyroxene-1	0.1214	0.0011	0.1697	0.0013	25.3	0.7	32.7	0.4	0.04	-5.2	1.58	0.27	**0.95**	0.16
3	Subhedral	Clinopyroxene-1	0.1215	0.0014	0.1710	0.0020	25.3	0.8	32.6	0.4	0.04	-5.1	1.56	0.32	**0.93**	0.19
4	Subhedral	Clinopyroxene-1	0.1233	0.0015	0.1694	0.0013	37.3	2.2	21.0	0.8	0.04	-3.8	1.14	0.35	**0.69**	0.21
5	Subhedral	Clinopyroxene-1	0.1234	0.0010	0.1700	0.0013	36.2	2.2	20.4	0.8	0.04	-3.7	**1.12**	0.23	**0.67**	0.14
7	Anhedral	Interstitial glass	0.1201	0.0008	0.1061	0.0005	79.0	8.8	11.7	1.1	0.02	-6.2	**1.50**	0.14	**1.12**	0.11
8	Anhedral	Interstitial glass	0.1201	0.0004	0.0641	0.0052	114.9	4.0	45.8	0.8	0.01	-6.3	***1.34***	0.06	***1.13***	0.05
9	Anhedral	Interstitial glass	0.1157	0.0005	0.1924	0.0034	59.4	1.4	4.2	0.1	0.04	-9.7	**3.17**	0.12	**1.74**	0.06
10	Anhedral	Interstitial glass	0.1153	0.0006	0.1928	0.0048	55.0	2.6	3.9	0.1	0.04	-10.0	**3.27**	0.17	**1.80**	0.09
11	Anhedral	Interstitial glass	0.1219	0.0006	0.2167	0.0084	62.5	0.8	35.9	0.3	0.05	-4.8	1.79	0.18	**0.87**	0.08
12	Anhedral	Interstitial glass	0.1245	0.0008	0.1609	0.0108	55.2	1.4	26.5	1.6	0.04	-2.8	0.83	0.19	0.52	0.12
13	Anhedral	Interstitial glass	0.1233	0.0005	0.2551	0.0066	77.4	6.0	3.2	0.1	0.06	-3.8	1.73	0.19	0.69	0.07
14	Anhedral	Interstitial glass	0.1234	0.0005	0.2534	0.0070	85.3	3.1	3.5	0.1	0.06	-3.7	1.66	0.19	0.67	0.07
15	Anhedral	Interstitial glass	0.1234	0.0005	0.2539	0.0064	79.9	5.2	3.3	0.1	0.06	-3.6	1.65	0.19	0.66	0.07
16	Anhedral	Interstitial glass	0.1170	0.0012	0.5049	0.0032	22.1	0.8	9.8	0.3	0.11	-8.7	-8.56	1.05	**1.57**	0.17
17	Anhedral	Interstitial glass	0.1177	0.0011	0.5039	0.0038	22.0	0.9	9.8	0.3	0.11	-8.1	-8.02	1.01	**1.46**	0.16
18	Anhedral	Interstitial glass	0.1258	0.0007	0.1778	0.0102	50.2	5.6	36.8	2.8	0.04	-1.8	0.58	0.16	0.33	0.09
Sample-72688																
1	Subhedral	Clinopyroxene-1	0.1265	0.0005	0.1887	0.0015	32.7	2.1	33.0	2.3	0.04	-1.3	**0.41**	0.14	**0.23**	0.08
2	Anhedral	Olivine	0.1261	0.0007	0.4317	0.0060	23.1	1.4	1.4	0.3	0.10	-1.6	-12.39	9.24	**0.28**	0.11
Sample-72689																
1	Anhedral	Interstitial glass	0.1261	0.0007	0.4317	0.0060	23.1	1.4	1.4	0.3	0.10	-1.6	-12.39	9.24	**0.28**	0.11
2	Anhedral	Interstitial glass	0.1243	0.0008	0.4394	0.0020	16.8	0.7	3.7	0.1	0.10	-2.9	-13.69	3.75	**0.53**	0.12
3	Anhedral	Interstitial glass	0.1251	0.0014	0.5131	0.0052	14.7	0.4	1.7	0.0	0.11	-2.3	-1.96	0.94	0.42	0.20
Sample-72690																
1	Subhedral	Olivine	0.1260	0.0012	0.0994	0.0014	45.5	10.8	62.6	6.9	0.02	-1.6	**0.39**	0.22	**0.30**	0.16
2	Subhedral	Intergranular	0.1211	0.0008	0.3344	0.0017	6.3	0.8	12.7	0.2	0.07	-5.4	4.65	0.51	0.99	0.11
3	Subhedral	Intergranular	0.1256	0.0005	0.2552	0.0024	29.9	1.6	26.9	2.0	0.06	-2.0	**0.90**	0.18	**0.36**	0.07
4	Anhedral	Interstitial glass	0.1237	0.0010	0.5718	0.0030	2.9	1.0	3.6	0.2	0.13	-3.5	-1.79	0.40	**0.63**	0.14
5	Subhedral	Interstitial glass	0.1193	0.0007	0.3160	0.0054	43.8	2.1	9.8	0.6	0.07	-6.8	4.81	0.42	1.24	0.09
Sample-72691																
1	Subhedral	Orthopyroxene	0.1194	0.0012	0.3585	0.0076	10.6	1.8	22.0	1.5	0.08	-6.8	7.83	1.34	**1.23**	0.16
2	Anhedral	Interstitial glass	0.1207	0.0009	0.1122	0.0034	25.6	0.6	1.5	0.1	0.02	-5.8	1.43	0.18	1.05	0.13
3	Anhedral	Interstitial glass	0.1149	0.0004	0.0456	0.0003	90.6	1.2	27.0	0.2	0.01	-10.3	***2.07***	0.07	***1.85***	0.06

4	Anhedral	Interstitial glass	0.1149	0.0007	0.0618	0.0005	61.5	2.0	10.1	0.3	0.01	-10.3	***2.17***	0.11	***1.86***	0.09
5	Anhedral	Interstitial glass	0.1147	0.0014	0.0237	0.0005	82.4	2.8	24.0	0.8	0.01	-10.5	***1.99***	0.21	***1.88***	0.20
6	Anhedral	Interstitial glass	0.1240	0.0008	0.2973	0.0036	41.9	1.4	11.5	0.3	0.07	-3.2	1.96	0.38	0.58	0.11
7	Anhedral	Interstitial glass	0.1236	0.0005	0.2189	0.0026	56.9	2.6	3.3	0.2	0.05	-3.5	1.34	0.15	0.64	0.07
8	Anhedral	Interstitial glass	0.1197	0.0010	0.1401	0.0011	33.7	2.2	10.8	0.4	0.03	-6.5	1.76	0.20	1.18	0.14
9	Anhedral	Interstitial glass	0.1240	0.0010	0.0944	0.0072	20.2	2.3	4.2	0.5	0.02	-3.2	0.74	0.19	0.58	0.14
10	Anhedral	Interstitial glass	0.1186	0.0013	0.0881	0.0016	41.0	0.6	7.4	0.2	0.02	-7.4	1.69	0.23	1.34	0.18
11	Anhedral	Interstitial glass	0.1222	0.0011	0.1039	0.0019	34.9	1.3	6.8	0.2	0.02	-4.6	1.10	0.20	0.83	0.15
12	Anhedral	Interstitial glass	0.1233	0.0008	0.1335	0.0030	21.6	1.2	4.6	0.2	0.03	-3.7	0.99	0.16	0.67	0.11
13	Anhedral	Interstitial glass	0.1213	0.0006	0.2983	0.0054	22.6	1.9	3.1	0.1	0.07	-5.3	3.25	0.31	0.97	0.08
14	Anhedral	Interstitial glass	0.1182	0.0006	0.1605	0.0026	25.5	5.2	6.8	0.5	0.04	-7.7	2.23	0.13	1.39	0.08
15	Anhedral	Interstitial glass	0.1212	0.0009	0.2329	0.0112	15.9	1.9	10.7	0.2	0.05	-5.4	2.16	0.30	0.97	0.13
16	Anhedral	Interstitial glass	0.1210	0.0012	0.3269	0.0038	16.7	0.8	23.5	0.7	0.07	-5.5	4.34	0.71	**1.00**	0.16
17	Anhedral	Interstitial glass	0.1241	0.0004	0.0942	0.0028	31.3	2.7	17.7	0.5	0.02	-3.1	0.73	0.07	0.57	0.06
18	Anhedral	Interstitial glass	0.1216	0.0005	0.1762	0.0038	25.4	2.8	7.8	0.2	0.04	-5.1	1.57	0.12	0.92	0.07
19	Anhedral	Interstitial glass	0.1233	0.0005	0.1578	0.0015	39.2	4.4	53.5	2.2	0.04	-3.7	1.08	0.11	0.68	0.07
20	Anhedral	Interstitial glass	0.1233	0.0004	0.1579	0.0014	40.0	4.0	54.3	2.2	0.04	-3.7	1.08	0.09	0.68	0.06
21	Anhedral	Interstitial glass	0.1234	0.0004	0.1564	0.0013	41.0	3.8	55.4	2.1	0.03	-3.7	1.06	0.08	0.67	0.05
22	Anhedral	Interstitial glass	0.1213	0.0007	0.2346	0.0022	20.0	1.0	2.3	0.2	0.05	-5.3	2.15	0.23	0.96	0.10
23	Anhedral	Interstitial glass	0.1203	0.0017	0.2472	0.0026	14.0	0.8	38.4	0.5	0.06	-6.1	2.64	0.56	1.10	0.24
Sample-111658																
1	Anhedral	Interstitial glass	0.1238	0.0008	0.2530	0.0076	60.1	2.9	12.6	0.4	0.06	-3.3	1.51	0.29	**0.61**	0.11
2	Anhedral	Interstitial glass	0.1242	0.0010	0.0756	0.0074	35.0	2.6	15.2	3.0	0.02	-3.0	0.67	0.17	**0.55**	0.14
Sample-111659																
1	Anhedral	Interstitial glass	0.1212	0.0013	0.0517	0.0015	104.4	8.0	10.9	0.8	0.01	-5.4	***1.11***	0.21	*0.97*	0.18
Sample-111664																
1	Anhedral	Interstitial glass	0.1257	0.0005	0.0819	0.0058	23.3	4.8	1.0	0.3	0.02	-1.9	***0.42***	0.10	***0.34***	0.08
2	Anhedral	Interstitial glass	0.1253	0.0004	0.0449	0.0008	48.2	16.8	11.7	4.0	0.01	-2.2	***0.44***	0.06	***0.39***	0.05
Sample-11165																
1	Anhedral	Interstitial glass	0.1219	0.0009	0.0232	0.0009	64.5	6.4	41.2	4.0	0.01	-4.8	***0.93***	0.13	***0.88***	0.13
2	Anhedral	Interstitial glass	0.1259	0.0009	0.1324	0.0028	42.3	3.2	6.1	0.5	0.03	-1.7	0.45	0.18	0.31	0.12
3	Anhedral	Interstitial glass	0.1233	0.0007	0.0121	0.0004	111.2	6.0	68.9	3.6	0.00	-3.8	***0.70***	0.10	***0.68***	0.10

(a, b) Seimiquantitative values: measured by comparison of signal with PGE-A stantard (Lorand and Alard, 2001)

(c, d, e) Calculated at basalt eruption age of 2Ma by comparison with Entastite Chondritic Reservoir (ECR; $^{187}Os/^{188}Os$ =0.1281 and $^{187}Re/^{188}Os$ =0.421; Walker et al., 2002)

(†) Propagated 2SE uncertainity of model ages calculated using Sambridge and Lambert (1997)

Lorand, J.-P., Alard, O., 2001, Platinum-group element abundances in the upper mantle: new constraints from in situ and whole-rock analyses of Massif Central xenoliths (France): Geochimica et Cosmochimica, v. Acta 65, p. 2789–2806.

Sambridge, M., Lambert, D.D., 1997, Propagating errors in decay equations: Examples from the Re-Os isotopic system: Geochimica et Cosmochimica Acta, v. 61,p. 3019-3024.

Walker, R.J., Horan, M.F., Morgan, J.W., Becker, H., Grossman, J.N., Rubin, A.E., 2002, Comparative ^{187}Re-^{187}Os systematics of chondrites: Implications regarding early solar system processes: Geochimica et Cosmochimica Acta, v. 66, p. 4187-4201.